Supplementary Information

Intermolecular Charge Transfer and Solid-state Solvent Effect Synergistically Induce Near-infrared Thermally Activated Delay Fluorescence in the Guest-Host System

Junfang Yang, Qian Peng*

School of Chemical Sciences, University of Chinese Academy of Sciences, Beijing 100049, P. R. China;

E-mail: qianpeng@ucas.ac.cn

Table of contents

1. Computational details

1.1 Calculation of dielectric constant

For the pure crystal state TPBi or TPAAP, The dielectric constant ε was evaluated via the Clausius-Mossotti relation,[1-2] which reads:

$$\frac{\varepsilon - 1}{\varepsilon + 2} = \frac{4\pi\alpha}{3\ V}$$

Here *V* is the volume occupied by a single molecule, which is obtained by applying the Multiwfn software.[3-4] The α term denotes the isotropic component of the molecular polarizability, which was calculated at the M06-2X/6-31G** level using the Gaussian 16 software.[5]

The resultant volume and polarizability were 420 Å^3 and 72.79 Å^3 for crystal state TPBi and 784 Å^3 and 78.37 Å^3 for crystal state TPAAP, respectively. And the calculated ε is 3.16 and 5.90 for TPBi and TPAAP, respectively. And the refractive index (n) of TPBi is about 1.73 from website, in terms of $n=\sqrt{\varepsilon}$, the ε is about 2.99, which is consistent with the calculated value.

For the 1 wt % and 20 wt % TPAAP: TPBi doping systems, the ε is calculated by the following relation:

$$\varepsilon = 1 + \frac{4\pi}{3}\frac{\langle|M|^2\rangle - |\langle M\rangle|^2}{\langle V\rangle k_B\langle T\rangle}$$

Here, k_B is the Boltzmann constants. The ***M*****,** *V* **and** *T* are the total dipole moment of the simulation box, the total volume of box, and the simulation temperature, which are obtained by MD simulations using GROMACS package. Thus, the calculated ε is 4.82 and 5.08 for 1 wt % and 20 wt % doping systems, respectively.

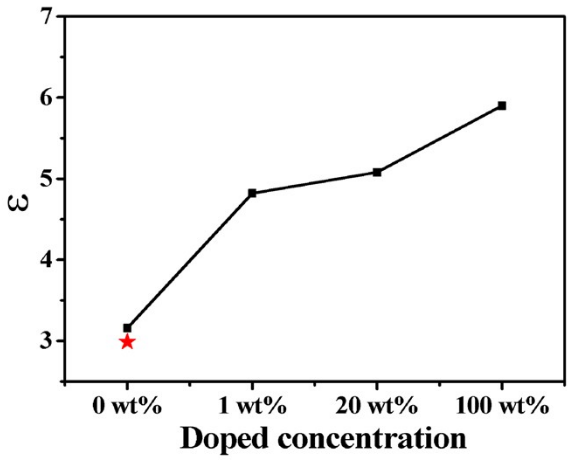

Figure S1. The calculated dielectric constant ε of different doping concentration and the experimental value is labeled by star.

1.2 Details of crystal simulation

To verify the reliability of MD simulation and determine the center of mass (COM) distance of TPAAP in the crystal, we performed MD simulations for TPAAP crystal. The parameters of TPAAP unit cell are a = 16.67 Å, b = 7.71 Å, c = 20.04 Å, α = 90.00, β = 107.51, γ = 90.00, which is from crystal data. We constructed the monoclinic supercell of TPAAP with size 5 × 5 × 5 nm^3 in the a, b, c dimensions by a replication of the original unit cell and then used this supercell as initial configuration for TPAAP crystal simulations. Furthermore, we performed energy minimization, followed by 2 ns equilibrium simulation under NVT (P = 1 bar and T = 300K) ensemble with temperature annealed from 50 to 300 K in the first 1 ns. Finally, we performed 20 ns MD simulations under NPT (P = 1 bar and T = 300 K) ensemble. The temperature and pressure ere controlled by the velocity rescaling thermostat[6] and Berendsen barostat[7-8], respectively. For the electrostatic interactions, the reciprocal space summation was evaluated by the particle mesh Ewald (PME) method[9-10]. The direct space summation was computed at a cutoff distance of 1.0 nm. The cutoff distance for VDW interactions was 0.9 nm. All bond lengths were constrained via the LINCS algorithm[11]. Periodic boundary condition was applied in all three directions to minimize the edge effects in a finite system. Here, the time step of the TPAAP supercell simulation was 0.2 fs. The configurations were stored at a time interval 20 ps for the COM distance of TPAAP calculations. In total, we collected 5000 MD conformations and calculated the COM distance of each conformation.

1.3 Quantum mechanics/molecular mechanics (QM/MM) model

The QM/MM calculations were performed by the ONIOM model in the Gaussian 16 package. The ONIOM models for the all systems were partitioned into two layers. The central molecules were selected as the high layer and calculated at ω*B97X-D/6-31G** level, while the surrounding molecules were set as the low layer and treated by a universal force field (UFF). The MM region mimics solid-state environment effects with the intermolecular electrostatic and van der Waals interactions. For the QM-monomer/MM of 1 wt % doped film, we chose one TPAAP in the middle as QM region, and other 63 molecules as MM region. For the QM-monomer/MM and QM-dimer/MM of 20 wt% doped film, the one and two TPAAP were chosen as QM region, the other 73 and 72 molecules as MM region, respectively.

1.4 Polarizable continuum model (PCM) model

The PCM model was implemented to describe solid-state solvent effect. The geometries of S_0, S_1 and T_1 of the guest-host systems were optimized using DFT and Tamm-Dancoff approximate (TDA) DFT with ω*B97X-D/6-31G**, and PCM is the linear response (LR) PCM model. Because of the serious CT feature in S_1 state with dipole moment of >35.0 Debye (35.67 Debye of 1 wt% and 35.80 Debye of 20 wt% doped systems), the state-specific PCM (SS-PCM)[12] were adopted to correct the energy of S_1, whose results are similar to the experiment value (Table S1).

Table S1. The energy of S_1 state by LR-PCM approach and corrected S_1 energy by SS-PCM approach.

	1 wt% Exp.(S_1)=648 nm	20 wt% Exp.(S_1)=711 nm	
	QM-monomer/PCM	QM-monomer/PCM	QM-dimer/PCM
LR-PCM	2.52 eV (491 nm)	2.52 eV (492 nm)	2.03 eV (609 nm)
SS-PCM	2.07 eV (600 nm)	2.06 eV (602 nm)	1.66 eV (747 nm)

1.5 Photophysical properties

The photoluminescence, prompt fluorescence, delayed fluorescence and intersystem crossing quantum efficiencies were calculated by the following formula:

$$\Phi_{PL} = \frac{k_r^S}{k_r^S + k_{IC}^S}$$

$$\Phi_{PF} = \frac{k_r^S}{k_r^S + k_{IC}^S + k_{ISC}}$$

$$\Phi_{TADF} = \Phi_{PL} - \Phi_{PF}$$

$$\Phi_{ISC} = \frac{k_{ISC}}{k_r^S + k_{IC}^S + k_{ISC}}$$

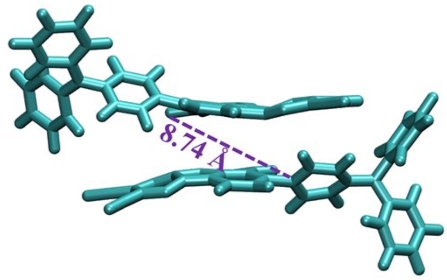

Figure S2. The chosen dimer from simulated configuration of 20 wt% doped film and corresponding center of mass distance is labeled.

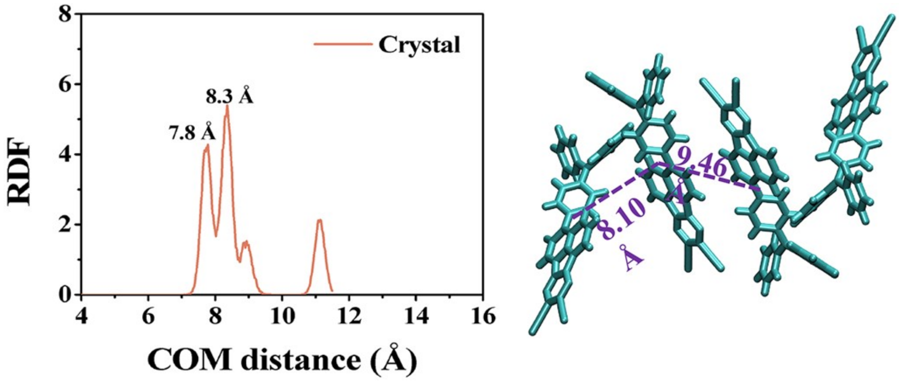

Figure S3. The RDFs as a function of center of mass (COM) distance between TPAAP molecules in crystal after MD simulation (left), and the measured COM distance between TPAAP in original crystal by using Mercury software (right).

The RDFs of crystal after MD simulation have a peak maximum at 8.3 Å for the first-neighbor shell, very close to the COM distance of adjacent molecules (8.1 Å) in X-ray crystal structure of TPAAP, which proves the reliability of the force field parameters and model adopted in this study.

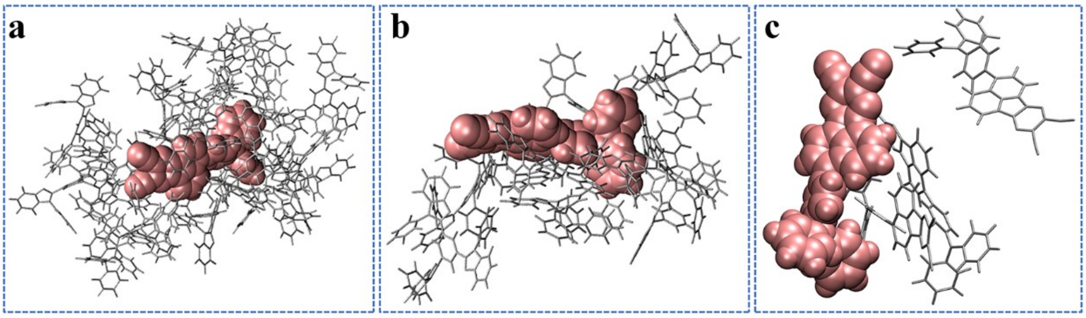

Figure S4. (a-b) Illustration of the local arrangements of neighboring TPBi molecules of a reference TPAAP molecule for 1 wt% and 20 wt% doping films, respectively. (c) Illustration of the local arrangements of neighboring TPAAP molecules of a reference TPAAP molecule for 20 wt% doping films.

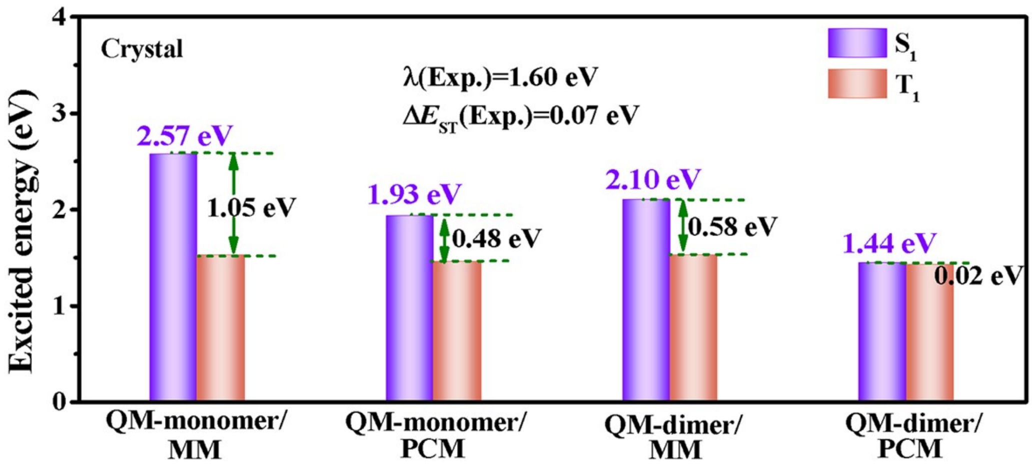

Figure S5. The 0-0 transition energies of the S_1 and T_1 and their energy gaps by using different computational models for TPAAP crystal.

Table S2. Important orbital transition properties for S_1 and T_1 states.

		S_1	T_1
1 wt%	QM-monomer	HOMO -> LUMO 82.3 % HOMO-1 -> LUMO 9.3 %	HOMO -> LUMO 63.8 % HOMO-1 -> LUMO 26.8 %
	QM-monomer/PCM	HOMO -> LUMO 84.8 % HOMO-1 -> LUMO 7.1 %	HOMO -> LUMO 66.5 % HOMO-1 -> LUMO 23.5%
	QM-monomer/MM	HOMO -> LUMO 81.5 % HOMO-1 -> LUMO 9.3 %	HOMO -> LUMO 56.0 % HOMO-1 -> LUMO 34.2 %
20 wt%	QM-monomer/PCM	HOMO -> LUMO 84.8 % HOMO-1 -> LUMO 7.1 %	HOMO -> LUMO 66.6 % HOMO-1 -> LUMO 23.4 %
	QM-monomer/MM	HOMO -> LUMO 82.4 % HOMO-1 -> LUMO 9.0 %	HOMO -> LUMO 44.1 % HOMO-1 -> LUMO 45.9 % HOMO -> LUMO+2 2.3 %
	QM-dimer/PCM	HOMO -> LUMO 96.2 %	HOMO -> LUMO 51.9 % HOMO-1 -> LUMO 15.5 % HOMO-2 -> LUMO 22.8 %
	QM-dimer/MM	HOMO -> LUMO 96.6 %	HOMO-1 -> LUMO 48.4 % HOMO-2 -> LUMO 40.3 % HOMO -> LUMO+4 2.3 %

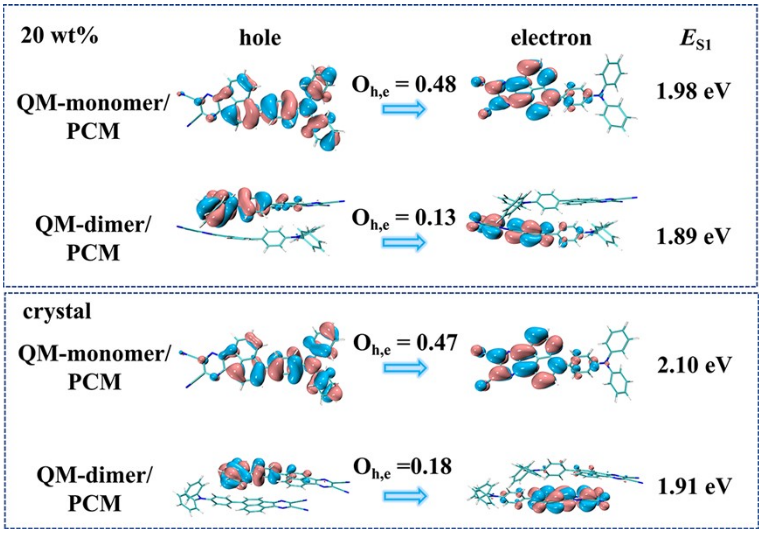

Figure S6 The natural transition orbitals (NTOs), the excitation energies of the S_1 and the overlap ($O_{h,e}$) between the hole and electron wavefunctions based on the optimized S_0 geometry in the 20 wt% doped films of TPAAP:TPBi and crystalline TPAAP.

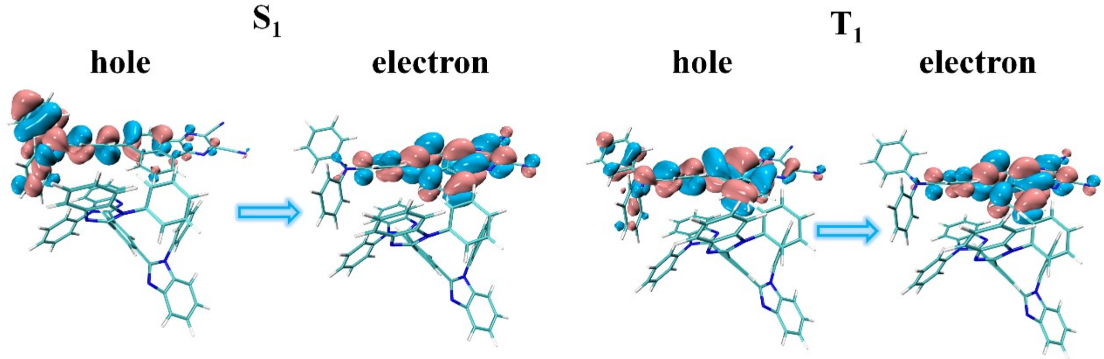

Figure S7. The NTOs of host-guest molecule at S_1 and T_1 states in 1 wt% doping film.

Table S3. The rate constants of the excited state decay processes, spin-orbit coupling (SOC), the photoluminescence quantum yield (Φ_{PL}), fluorescence quantum yield (Φ_{PF}) and TADF yield (Φ_{TADF}) calculated by QM-monomer/PCM, QM-monomer/MM and QM-dimer/PCM models for 1 wt% and 20 wt% doped films.

		k_r^S (s^{-1})	k_{IC}^S (s^{-1})	$SOC_{S_1T_1}$ (cm^{-1})	k_{ISC} (s^{-1})	k_{rISC} (s^{-1})	Φ_{PL}	Φ_{PF}	Φ_{TADF}
1 wt%	QM-monomer/PCM	2.01×10^8 (9.49×10^7)	6.27×10^5 (2.23×10^5)	0.148	5.21×10^6 (8.17×10^5)	1.13×10^5	99.7% (97.7%)	97.2%	2.5% (7.58%)
20 wt%	QM-monomer/PCM	2.00×10^8	6.09×10^5	0.149	4.85×10^6	1.56×10^6	98.1%	97.3%	0.8%
	QM-dimer/PCM	4.82×10^6 (3.35×10^7)	5.63×10^6 (2.21×10^6)	0.195	8.31×10^6 (5.91×10^5)	2.63×10^5	46.1% (60.3%)	25.7%	20.4% (5.79%)

Table S4 The geometrical coordinates of in the S_0 at QM-monomer/PCM model for 1 wt% doped film.

Atom	x (Å)	y (Å)	z (Å)
N	-6.055573	1.538512	-0.244741
N	4.873974	0.101956	-0.028767
N	-6.544813	-1.251274	0.169447
N	-9.280669	2.674593	-0.464147
C	5.510829	-1.158866	-0.177451
C	-5.079794	0.660027	-0.097802
C	-3.061478	-0.405679	0.093859
C	-3.637437	0.871289	-0.105403
C	-5.327269	-0.744508	0.112811
C	5.673956	1.267878	0.108317
C	3.470313	0.195870	-0.023696
C	2.818048	1.152116	0.770390
H	3.401285	1.817142	1.397194
C	-0.827225	0.500951	-0.012561
C	0.647801	0.378682	-0.007245
C	-7.296513	1.017554	-0.186384
C	1.433728	1.245715	0.765364
H	0.951118	1.981897	1.400873
C	-4.038934	-1.419995	0.242960
C	-7.537584	-0.352829	0.015570
C	-2.808649	1.964376	-0.237745
H	-3.203917	2.962863	-0.388315
C	-1.681016	-0.641726	0.159887
N	-9.971674	-1.261037	0.107959
C	5.062850	-2.270319	0.547291
H	4.223443	-2.162884	1.226159
C	2.691431	-0.662868	-0.814861
H	3.177020	-1.392599	-1.452844
C	1.306544	-0.576429	-0.795997
H	0.729832	-1.233504	-1.439380
C	-1.412694	1.754272	-0.191280
H	-0.759300	2.608995	-0.331256
C	5.371958	2.425475	-0.619519
H	4.519997	2.427674	-1.291134
C	6.602807	-1.296918	-1.042628
H	6.949848	-0.436648	-1.605040
C	6.781333	1.263067	0.964803
H	7.015112	0.366831	1.529566

C	-1.300044	-1.985264	0.433372
H	-0.251236	-2.237371	0.542813
C	-2.253772	-2.978697	0.579987
H	-1.927941	-3.991555	0.789209
C	-3.641992	-2.717777	0.479834
H	-4.362530	-3.518825	0.601893
C	-8.392507	1.938313	-0.340750
C	7.238489	-2.528369	-1.173672
H	8.085102	-2.621718	-1.846134
C	5.691256	-3.502870	0.394183
H	5.333770	-4.356984	0.960275
C	6.160237	3.564007	-0.478379
H	5.914852	4.455489	-1.046487
C	-8.883685	-0.859830	0.067584
C	6.783962	-3.638358	-0.462079
H	7.276840	-4.598340	-0.572188
C	7.576641	2.399342	1.083676
H	8.433669	2.382435	1.749141
C	7.268198	3.556554	0.368850
H	7.885583	4.442731	0.469705

Table S5 The geometrical coordinates of in the S_0 by QM-dimer/PCM model for 20 wt% doped film.

Atom	x (Å)	y (Å)	z (Å)
N	-6.865049	0.024185	1.096597
N	4.009048	0.800988	2.207656
N	-6.861777	-2.832128	1.262749
N	-10.089841	0.557815	0.083510
C	4.448014	2.151241	2.336408
C	-5.788199	-0.666990	1.420479
C	-3.653417	-1.355135	1.872425
C	-4.440989	-0.192437	1.701438
C	-5.783666	-2.106074	1.486542
C	4.963887	-0.232507	2.075913
C	2.623167	0.547859	2.217293
C	1.773758	1.310563	3.034332
H	2.195480	2.069236	3.683872
C	-1.640239	-0.048188	2.123781
C	-0.173255	0.115241	2.203275
C	-7.954512	-0.720955	0.831888

C	0.402815	1.100108	3.019012
H	-0.229043	1.693434	3.672600
C	-4.420855	-2.542151	1.780169
C	-7.957577	-2.122634	0.929024
C	-3.838518	1.041684	1.806868
H	-4.398349	1.963411	1.694854
C	-2.268612	-1.340350	2.092213
N	-10.118144	-3.469136	0.405425
C	5.379190	2.505438	3.317453
H	5.769029	1.743026	3.983523
C	2.056127	-0.440525	1.402575
H	2.691248	-1.031387	0.753736
C	0.685092	-0.649720	1.399491
H	0.272754	-1.385066	0.716861
C	-2.444757	1.085799	2.021802
H	-1.963972	2.057393	2.051877
C	4.703707	-1.526188	2.552554
H	3.753136	-1.746118	3.025032
C	3.938822	3.130633	1.477851
H	3.218214	2.845367	0.718323
C	6.212813	0.033042	1.493812
H	6.432360	1.025444	1.117222
C	-1.664337	-2.614363	2.283607
H	-0.605724	-2.682131	2.507707
C	-2.414603	-3.775994	2.206584
H	-1.921823	-4.729468	2.361159
C	-3.805403	-3.764160	1.940155
H	-4.361443	-4.692922	1.877131
C	-9.136445	-0.010345	0.421652
C	4.354508	4.453136	1.604330
H	3.953723	5.206975	0.934469
C	5.805111	3.826693	3.426037
H	6.530938	4.093083	4.187251
C	5.661510	-2.528028	2.428316
H	5.435096	-3.523211	2.797336
C	-9.152314	-2.871689	0.643584
C	5.292703	4.805528	2.574442
H	5.622397	5.834854	2.666132
C	7.178287	-0.966131	1.417714
H	8.151077	-0.729031	0.999313
C	6.908681	-2.257208	1.867638
H	7.659652	-3.035430	1.789147
N	6.977079	0.438179	-1.887617

N	-4.011699	1.446045	-1.872694
N	6.775336	-2.416171	-1.784363
N	10.385675	0.783265	-1.901256
C	-4.864431	0.324134	-2.016902
C	5.817216	-0.192597	-1.853762
C	3.598494	-0.760397	-1.881393
C	4.467033	0.356303	-1.879464
C	5.717352	-1.628792	-1.806166
C	-4.558777	2.724862	-1.577740
C	-2.609536	1.288596	-1.931673
C	-2.022553	0.425813	-2.868378
H	-2.648331	-0.091135	-3.587132
C	1.648070	0.657385	-1.942901
C	0.186672	0.883821	-1.963614
C	8.055046	-0.368263	-1.863885
C	-0.649571	0.221730	-2.874733
H	-0.218275	-0.437301	-3.621554
C	4.301905	-1.987628	-1.809316
C	7.956836	-1.769904	-1.809464
C	3.925249	1.622416	-1.886706
H	4.549779	2.508648	-1.874492
C	2.200409	-0.667887	-1.914714
N	10.100959	-3.237139	-1.728267
C	-4.460418	-0.944564	-1.578831
H	-3.485130	-1.072432	-1.123049
C	-1.774300	1.985464	-1.048037
H	-2.210136	2.671194	-0.332048
C	-0.401898	1.783899	-1.064825
H	0.218832	2.295407	-0.335637
C	2.517735	1.746537	-1.917468
H	2.090359	2.743502	-1.947444
C	-5.610038	2.861750	-0.661838
H	-6.029053	1.983436	-0.180336
C	-6.135751	0.469416	-2.590512
H	-6.458222	1.442791	-2.942310
C	-4.043862	3.865086	-2.206447
H	-3.239137	3.761062	-2.926562
C	1.501369	-1.905233	-1.839968
H	0.417251	-1.913973	-1.829941
C	2.186664	-3.105552	-1.755754
H	1.621277	-4.028483	-1.690541
C	3.601512	-3.171529	-1.744480
H	4.107662	-4.127848	-1.676091

C	9.343413	0.273596	-1.888304
C	-6.988491	-0.624553	-2.697128
H	-7.972623	-0.488261	-3.133282
C	-5.310276	-2.038288	-1.715350
H	-4.978419	-3.011519	-1.368149
C	-6.130342	4.122453	-0.382120
H	-6.947501	4.212051	0.326392
C	9.141441	-2.585933	-1.768609
C	-6.583607	-1.886788	-2.263143
H	-7.247705	-2.739477	-2.354253
C	-4.557397	5.123394	-1.904657
H	-4.145622	5.998197	-2.397477
C	-5.604331	5.260153	-0.993787
H	-6.008847	6.240796	-0.767348

References:

S1. Nayak, P. K.; Periasamy, N., Calculation of ionization potential of amorphous organic thin-films using solvation model and DFT. *Organic Electronics* **2009,** *10* (3), 532.

S2. Solid State Physics. Von N. W. Ashcroft und N. D. Mermin; Holt, Rinehart and Winston, New York 1976, XXII, 826 Seiten, $19,95. *Physik in unserer Zeit* **1978,** *9* (1), 33.

S3. Lu, T.; Chen, F., Multiwfn: A multifunctional wavefunction analyzer. *Journal of Computational Chemistry* **2012,** *33* (5), 580.

S4. Guido, C. A.; Cortona, P.; Mennucci, B.; Adamo, C., On the Metric of Charge Transfer Molecular Excitations: A Simple Chemical Descriptor. *Journal of Chemical Theory and Computation* **2013,** *9* (7), 3118.

S5. M. J. Frisch, G. W. T., H. B. Schlegel, G. E. Scuseria, M. A. Robb, J. R. Cheeseman, G. Scalmani, V. Barone, G. A. Petersson, H. Nakatsuji, X. Li, M. Caricato, A. V. Marenich, J. Bloino, B. G. Janesko, R. Gomperts, B. Mennucci, H. P. Hratchian, J. V. Ortiz, A. F. Izmaylov, J. L. Sonnenberg, D. Williams-Young, F. Ding, F. Lipparini, F. Egidi, J. Goings, B. Peng, A. Petrone, T. Henderson, D. Ranasinghe, V. G. Zakrzewski, J. Gao, N. Rega, G. Zheng, W. Liang, M. Hada, M. Ehara, K. Toyota, R. Fukuda, J. Hasegawa, M. Ishida, T. Nakajima, Y. Honda, O. Kitao, H. Nakai, T. Vreven, K.

Throssell, J. A. Montgomery, Jr., J. E. Peralta, F. Ogliaro, M. J. Bearpark, J. J. Heyd, E. N. Brothers, K. N. Kudin, V. N. Staroverov, T. A. Keith, R. Kobayashi, J. Normand, K. Raghavachari, A. P. Rendell, J. C. Burant, S. S. Iyengar, J. Tomasi, M. Cossi, J. M. Millam, M. Klene, C. Adamo, R. Cammi, J. W. Ochterski, R. L. Martin, K. Morokuma, O. Farkas, J. B. Foresman, and D. J. Fox., Gaussian16 Revision A.03. Gaussian Inc. Wallingford CT. **2016**.

S6. Bussi, G.; Donadio, D.; Parrinello, M., Canonical sampling through velocity rescaling. *J. Chem. Phys.* **2007,** *126* (1), 014101.

S7. Berendsen, H. J. C.; Postma, J. P. M.; van Gunsteren, W. F.; Hermans, J., Interaction Models for Water in Relation to Protein Hydration. In *Intermolecular Forces: Proceedings of the Fourteenth Jerusalem Symposium on Quantum Chemistry and Biochemistry Held in Jerusalem, Israel, April 13–16, 1981*, Pullman, B., Ed. Springer Netherlands: Dordrecht, 1981; 331.

S8. Berendsen, H. J. C.; Postma, J. P. M.; Gunsteren, W. F. v.; DiNola, A.; Haak, J. R., Molecular dynamics with coupling to an external bath. *The Journal of Chemical Physics* **1984,** *81* (8), 3684-3690.

S9. Essmann, U.; Perera, L.; Berkowitz, M. L.; Darden, T.; Lee, H.; Pedersen, L. G., A smooth particle mesh Ewald method. *The Journal of Chemical Physics* **1995,** *103* (19), 8577.

S10. York, D. M.; Darden, T. A.; Pedersen, L. G., The effect of long-range electrostatic interactions in simulations of macromolecular crystals: A comparison of the Ewald and truncated list methods. *The Journal of Chemical Physics* **1993,** *99* (10), 8345.

S11. Hess, B.; Bekker, H.; Berendsen, H. J. C.; Fraaije, J. G. E. M., LINCS: A linear constraint solver for molecular simulations. *Journal of Computational Chemistry* **1997,** *18* (12), 1463-1472.

S12. Guido, C. A.; Mennucci, B.; Scalmani, G.; Jacquemin, D., Excited State Dipole Moments in Solution: Comparison between State-Specific and Linear-Response TD-DFT Values. *Journal of Chemical Theory and Computation* **2018,** *14* (3), 1544.